Reversal of hyperactive subthalamic circuits differentially mitigates pain hypersensitivity phenotypes in parkinsonian mice

Yiwen Luan[a,1], Dongliang Tang[a,1], Haichuan Wu[a,1], Weixin Gu[a], Yuqing Wu[a,b], Jun-Li Cao[a,b,2], Cheng Xiao[a,b,2], and Chunyi Zhou[a,b,2]

[a]School of Anesthesiology, Xuzhou Medical University, Xuzhou, Jiangsu 221004, China; and [b]Jiangsu Province Key Laboratory of Anesthesiology, Xuzhou Medical University, Xuzhou, Jiangsu 221004, China

Edited by Bernardo L. Sabatini, Harvard Medical School, Boston, MA, and approved March 23, 2020 (received for review September 20, 2019)

Although pain is a prevalent nonmotor symptom in Parkinson's disease (PD), it is undertreated, in part because of our limited understanding of the underlying mechanisms. Considering that the basal ganglia are implicated in pain sensation, and that their synaptic outputs are controlled by the subthalamic nucleus (STN), we hypothesized that the STN might play a critical role in parkinsonian pain hypersensitivity. To test this hypothesis, we established a unilateral parkinsonian mouse model with moderate lesions of dopaminergic neurons in the substantia nigra. The mice displayed pain hypersensitivity and neuronal hyperactivity in the ipsilesional STN and in central pain-processing nuclei. Optogenetic inhibition of STN neurons reversed pain hypersensitivity phenotypes in parkinsonian mice, while hyperactivity in the STN was sufficient to induce pain hypersensitivity in control mice. We further demonstrated that the STN differentially regulates thermal and mechanical pain thresholds through its projections to the substantia nigra pars reticulata (SNr) and the internal segment of the globus pallidus (GPi)/ventral pallidum (VP), respectively. Interestingly, optogenetic inhibition of STN-GPi/STN-VP and STN-SNr projections differentially elevated mechanical and thermal pain thresholds in parkinsonian mice. In summary, our results support the hypothesis that the STN and its divergent projections play critical roles in modulating pain processing under both physiological and parkinsonian conditions, and suggest that inhibition of individual STN projections may be a therapeutic strategy to relieve distinct pain phenotypes in PD.

subthalamic nucleus | Parkinson's disease | pain hypersensitivity | central pain processing | optogenetics

Pain is a prevalent and distressing nonmotor symptom of Parkinson's disease (PD), affecting 30 to 95% of patients, but effective treatment of PD pain has been hindered by our limited understanding of the underlying mechanisms (1–4). Pathophysiological dopamine depletion in the basal ganglia due to the death of dopaminergic (DA) neurons in the substantia nigra pars compacta (SNc) is related to the motor symptoms of PD (5, 6). Because the therapeutic efficacy of dopamine drugs in relieving the diverse set of pain symptoms associated with PD is inconsistent (2, 7–10), pathophysiological processes other than dopamine depletion may be involved in pain symptoms in PD.

PD patients and parkinsonian animal models exhibit accelerated and irregular neuronal firing and abnormal oscillations in the local field potential in the basal ganglia nuclei, including the subthalamic nucleus (STN), globus pallidus interna (GPi), and substantia nigra pars reticulata (SNr), and these abnormalities are correlated with motor deficits (11–17). As the substantia nigra, striatum, and globus pallidus integrate nociceptive information to render pain avoidance and nocifensive behaviors (2, 10, 18), neural circuit dysfunction in these regions may lead to the hyperalgesia and shortened nociceptive reflex latencies observed in parkinsonian animal models (19–23). However, addressing the gap between the dysfunction in basal ganglia circuits and pain sensitization in PD requires experiments using sophisticated neuromodulation techniques.

In the basal ganglia, the STN sends glutamatergic projections to the SNr and GPi, the two output nuclei (16, 24, 25). Although abnormal activity in the STN plays a critical role in parkinsonian motor deficits (16, 26), its association with pain symptoms in PD has not been well studied. An in vivo electrophysiological study revealed that STN neurons have faster spontaneous firing and stronger responses to nociceptive stimuli in parkinsonian rats compared with control rats (27). Deep brain stimulation (DBS) in patients with PD effectively relieves musculoskeletal and dystonic pain, but not central or neuropathic pain (28–32). The aforementioned evidence hints that the STN may play significant roles in pain perception and modulation; however, cell- and projection-specific neuromodulation of STN neurons and axonal projections without perturbation of other circuit components are needed to clarify whether the abnormal activity in the STN is the key pathophysiology that underlies pain symptoms in PD. Answering this question may advance our understanding of how the basal ganglia circuits regulate pain perception, and which parts

Significance

Treatments for pain symptoms in patients with Parkinson's disease (PD) show inconsistent efficacy across clinical trials, largely owing to our limited understanding of the mechanisms underlying PD pain. Here, we demonstrate that overactivation of subthalamic nucleus (STN) neurons and their projections is adequate to produce a pain hypersensitivity phenotype, and that such overactivation is essential for the hypersensitivity in pain processing pathways and the maintenance of pain hypersensitivity observed in parkinsonian mice. These results suggest that inhibition of STN neurons may be a potential therapeutic strategy for pain relief in PD. Our finding that individual STN projections differentially regulate mechanical and thermal pain thresholds raises the possibility that individual STN projections may be optimal therapeutic targets for different pain phenotypes.

Author contributions: J.-L.C., C.X., and C.Z. designed research; Y.L., D.T., H.W., W.G., C.X., and C.Z. performed research; Y.L., D.T., Y.W., C.X., and C.Z. analyzed data; and J.-L.C., C.X., and C.Z. wrote the paper.

The authors declare no competing interest.

This article is a PNAS Direct Submission.

[1]Y.L., D.T., and H.W. contributed equally to this work.

[2]To whom correspondence may be addressed. Email: caojl0310@aliyun.com, xchengxj@xzhmu.edu.cn, or 100002016033@xzhmu.edu.cn.

This article contains supporting information online at https://www.pnas.org/lookup/suppl/doi:10.1073/pnas.1916263117/-/DCSupplemental.

First published April 20, 2020.

of this circuitry are suitable candidate targets for the treatment of pain symptoms in PD.

In the present study, we established a partial parkinsonian mouse model by unilateral injection of 6-hydroxydopamine (6-OHDA) into the medial forebrain bundle (MFB) to moderately lesion SNc DA neurons (33, 34). We used optogenetic techniques to bidirectionally modulate STN neurons and their axonal projections, which was confirmed by neuronal tracing and electrophysiological recordings. Our results support the hypothesis that STN neurons and their distinct projections are implicated in pain hypersensitivity in parkinsonian mice, and suggest that diverse pain symptoms in PD may be relieved by selective modulation of distinct STN projections.

Results

Unilateral Lesion of SNc DA Neurons Leads to Mechanical and Thermal Hypersensitivity. To establish a parkinsonian mouse model, we microinjected 6-OHDA into the MFB in the right hemisphere of the mouse brain (Fig. 1 *A* and *B*) to unilaterally lesion SNc DA neurons. From a week after the 6-OHDA injection onward, we observed a 50 to 60% loss of SNc DA neurons on the lesioned side (Fig. 1 *C* and *D*; *SI Appendix*, Fig. S1 *A–D* and Table S1), and the mice exhibited a 20 to 40% deficit in the distance traveled in an open field arena. Motor function was mildly impaired at 7 d after the 6-OHDA lesion and showed partial recovery at 14 and 25 d after the lesion (Fig. 1*E*).

To obtain information about the development of pain hypersensitivity in parkinsonian mice under our experimental conditions, we measured the mechanical (Fig. 1*F*) and thermal (Fig. 1*G*) pain thresholds in both ipsilesional and contralesional hindpaws after 6-OHDA injection (Fig. 1*B*). Parkinsonian mice displayed robust mechanical hypersensitivity in both ipsilesional and contralesional hindpaws at 7 d after 6-OHDA injection, and this hypersensitivity was maintained at similar levels until at least 28 d after 6-OHDA injection (Fig. 1*F*). The parkinsonian mice also exhibited thermal hypersensitivity on both hindpaws, with progression similar to that of mechanical hypersensitivity (Fig. 1*G*). Although parkinsonian mice had a minor deficit in voluntary movement (Fig. 1*E*), they did not show any deficits in the hindpaw tape-removal test, which involves lifting the hindpaw on sensory stimulation (*SI Appendix*, Fig. S2).

To address whether the pain hypersensitivity observed in parkinsonian mice is associated with dopamine depletion, we intraperitoneally injected levodopa (L-dopa; 0.5 mg/kg) and measured pain thresholds after 1 h (Fig. 1 *H* and *I*). We observed that L-dopa significantly elevated the mechanical and thermal pain thresholds in both hindpaws of parkinsonian mice.

These data indicate that unilateral lesion of SNc DA neurons induces bilateral mechanical and thermal hypersensitivity, and that the development of pain hypersensitivity concurs with the loss of SNc DA neurons.

Enhanced Excitability of STN Neurons Contributes to Pain Hypersensitivity in Parkinsonian Mice. Hyperactivity in multiple nuclei in the basal ganglia has been reported in PD patients and animal models (12–14, 16, 17). To confirm that STN neurons are hyperactive in our parkinsonian mice, we performed brain-slice patch-clamp recordings from STN neurons in both hemispheres of parkinsonian and control mice (Fig. 2*A*). We observed that the spontaneous firing rates of STN neurons were significantly higher on the ipsilesional side than on either the contralesional side or in control mice (Fig. 2*B*); on injection of depolarizing current steps, the firing rates of STN neurons were enhanced the most on the ipsilesional side, followed by the contralesional side and then the saline injection side (in control mice) (Fig. 2*C*). Therefore, 6-OHDA lesion of SNc DA neurons enhanced the baseline activity in ipsilesional STN neurons, but enhanced evoked activity in both ipsilesional and contralesional STN neurons.

Considering that STN neurons respond to nociceptive stimuli (27, 35), and that STN DBS effectively relieves pain symptoms in some PD patients (28, 30, 32), we wondered whether the hyperactivity in STN neurons contributes to pain hypersensitivity in parkinsonian mice. To investigate this, we injected adeno-associated virus (AAV)-CaMKII-NpHR3.0-eYFP into the STN (Fig. 2*D*) to achieve optogenetic inhibition of STN neurons (*SI Appendix*, Fig. S3 *A–D*). At 2 wk after unilateral 6-OHDA lesioning (Fig. 2 *E* and *F*), optogenetic inhibition of ipsilesional STN neurons elevated both the mechanical (Fig. 2*G*) and thermal (Fig. 2*H*) pain thresholds in STN CaMKII-NpHR mice; however, ipsilesional yellow light illumination changed neither the mechanical (Fig. 2*I*) nor the thermal (Fig. 2*J*) pain threshold in unilateral 6-OHDA–lesioned mice that received a control AAV-CaMKII-eYFP injection in the ipsilesional STN. These data indicate that inhibition of STN neurons reverses pain hypersensitivity in parkinsonian mice. It is possible that the observed changes in pain thresholds may be due to exacerbation of motor deficits, leading to delayed nocifensive responses; however, this is unlikely, given that photoinhibition of STN neurons did not alter mobility in parkinsonian mice (*SI Appendix*, Fig. S3 *E* and *F*).

In control mice subjected to saline injection in the MFB, the surgical procedure did not alter the mechanical or thermal pain thresholds and optogenetic inhibition of STN neurons did not modulate pain thresholds (*SI Appendix*, Fig. S3 *G–J*). One explanation for this is that the control mice lack the increase in spontaneous STN activity observed in parkinsonian mice, which may sensitize central pain pathways. Thus, inhibition of the STN may alter the pain thresholds in parkinsonian mice by mitigating a hypersensitive state. To test this, we performed the next set of experiments.

Multiple Pain-Processing Nuclei Are Involved in Pain Hypersensitivity in Parkinsonian Mice. Given that PD patients with lower pain thresholds show overactivation of the anterior cingulate cortex, prefrontal cortex, and insular cortex (7), we wondered whether the reduced pain thresholds in parkinsonian mice are related to hyperactivity in these regions, and whether STN photoinhibition could reverse hyperactivity in these regions. To answer these questions, we analyzed c-fos expression in these cortical areas in mice subjected to unilateral saline injection in the MFB (Saline group), 6-OHDA injection in the MFB (6-OHDA group), or 6-OHDA injection in the MFB plus optogenetic inhibition of ipsilesional STN neurons [6-OHDA+STN(−) group]. As illustrated in Fig. 3, we observed more c-fos–positive neurons in the anterior cingulate cortex (Fig. 3 *A–D*), prefrontal cortex (Fig. 3 *E–H*), and insular cortex (Fig. 3 *I–L*) in 6-OHDA mice than in Saline mice, and the increase in the number of c-fos–positive neurons in 6-OHDA mice was reversed by optogenetic inhibition of STN neurons.

We also counted c-fos–positive neurons in the parabrachial nucleus (PBN), a brainstem nucleus participating in the relay of pain signals, and found that the number of c-fos–positive neurons in the PBN was increased in 6-OHDA mice relative to Saline mice, but that this increase was reversed in 6-OHDA+STN(−) mice (Fig. 3 *M–P*).

These results suggest that hyperactivity in STN neurons may sensitize central pain processing, thereby leading to the pain hypersensitivity observed in parkinsonian mice.

Selective Stimulation of STN Neurons Reduces Pain Thresholds in Mice. The parkinsonian mice used in the foregoing above experiments showed both lesioning of SNc DA neurons (Fig. 1 *C* and *D*) and hyperactivity in STN neurons (Fig. 2 *B* and *C*). It is possible that the increased pain sensitivity may be due to an interaction between these two factors. To address whether elevated activity in STN neurons alone induces a reduction in pain

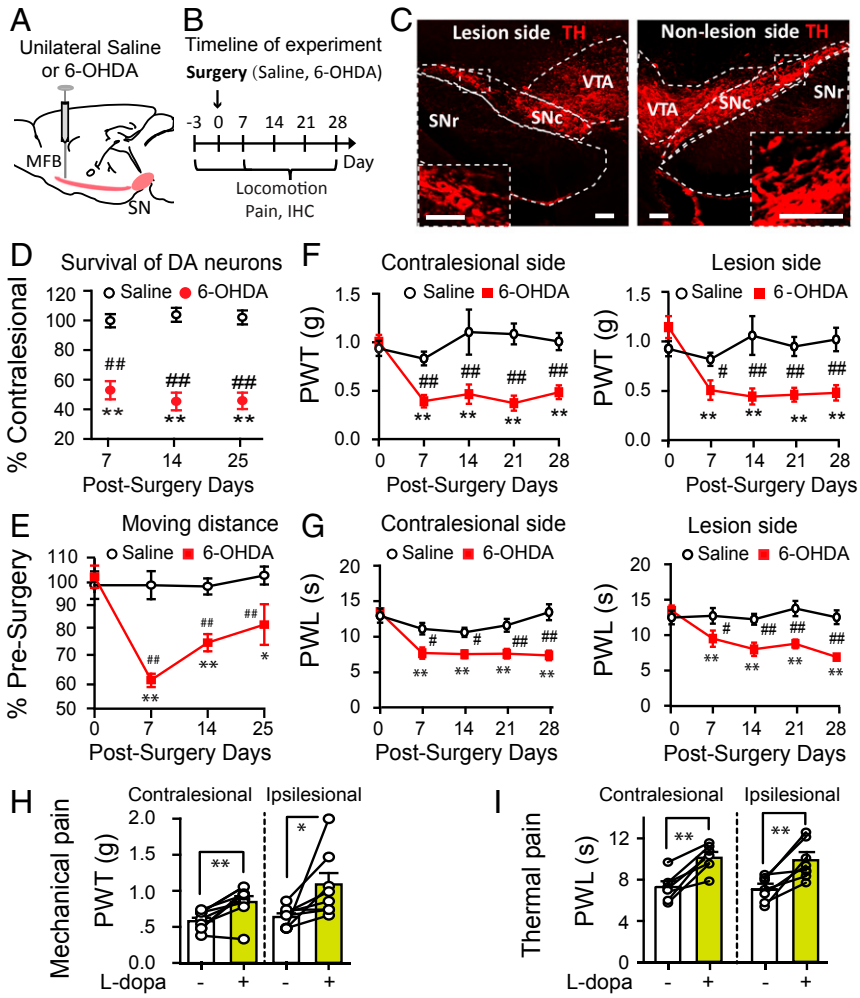

Fig. 1. Unilateral parkinsonian mice exhibit mechanical and thermal pain hypersensitivity. (*A*) Diagram showing stereotactic microinjection of 6-OHDA into the right MFB to establish a unilateral parkinsonian mouse model. (*B*) Timeline of experiments. (*C*) Representative images showing unilateral lesion of SNc DA neurons (*Right*). (Scale bar: 100 μm.) (*D*) Reduction of SNc DA neurons after 6-OHDA injections (two-way ANOVA: $F = 249.3$, $P < 0.001$; contralesional vs. ipsilesional, $t = 15.8$, $P < 0.001$; $n = 7$ to 9). (*E*) Change in locomotion after unilateral 6-OHDA lesion ($n = 10$; two-way ANOVA; postsurgery days, $F = 7.61$, $P < 0.001$; Saline vs. 6-OHDA, $F = 32.74$, $P < 0.001$; interaction between postsurgery days and Saline/6-OHDA, $F = 7.06$, $P < 0.001$). (*F*) Mechanical pain thresholds were measured with von Frey filaments. Unilateral 6-OHDA lesioned mice displayed bilateral mechanical pain hypersensitivity. (*Left*) Contralesional hindpaw, $n = 8$; two-way ANOVA: Saline vs. 6-OHDA, $F = 47.97$, $P = 0.001$; postsurgery days, $F = 3.07$, $P = 0.023$; interaction between postsurgery days and Saline/6-OHDA, $F = 4.41$, $P = 0.004$. (*Right*) Ipsilesional hindpaw, $n = 8$; two-way ANOVA: Saline vs. 6-OHDA, $F = 26.1$, $P < 0.001$; postsurgery days, $F = 4.04$, $P = 0.006$; interaction between postsurgery days and Saline/6-OHDA, $F = 5.25$, $P = 0.001$. (*G*) Thermal pain thresholds were determined with a plantar anesthesia tester. Unilateral 6-OHDA lesioned mice displayed bilateral thermal pain hypersensitivity. (*Left*) Contralesional hindpaw, $n = 8$; two-way ANOVA: Saline vs. 6-OHDA, $F = 40.35$, $P < 0.001$; postsurgery days, $F = 9.71$, $P < 0.001$; interaction between postsurgery days and Saline/6-OHDA, $F = 5.03$, $P = 0.002$. (*Right*) Ipsilesional hindpaw, $n = 8$; two-way ANOVA: Saline vs. 6-OHDA, $F = 33.9$, $P < 0.001$; postsurgery days, $F = 3.93$, $P = 0.007$; interaction between postsurgery days and Saline/6-OHDA, $F = 4.19$, $P = 0.005$. (*H* and *I*) Effects of intraperitoneal injection of 0.5 mg/kg L-dopa on mechanical pain (*H*) and thermal pain (*I*) thresholds on both hindpaws of parkinsonian mice. In H, contralesional side: $t = -4.12$, $P = 0.004$; ipsilesional side: $t = -2.67$, $P = 0.03$; $n = 8$, paired t test. In *I*, contralesional side: $t = -5.76$, $P = 0.001$; ipsilateral side: $t = -4.41$, $P = 0.001$; $n = 8$, paired t test. In *D*–*G*, $^{**}P < 0.01$ compared with presurgery baseline levels; $^{\#\#}P < 0.01$ compared with Saline. In *H* and *I*, $^{*}P < 0.05$; $^{**}P < 0.01$ compared with pre–L-dopa treatment.

thresholds, we performed unilateral optogenetic stimulation of STN neurons in control mice (Fig. 4 *A* and *B*). We confirmed the efficacy of the optogenetic stimulation with ex vivo brain slice patch-clamp recordings (Fig. 4*C*) and c-fos staining in brain sections from mice subjected to in vivo photostimulation of STN neurons (Fig. 4 *D* and *E*). After confirming that photostimulation of STN neurons did not alter the mobility of mice within the chambers that were used for measuring the pain thresholds (*SI Appendix*, Fig. S4 *A*–*D*), we measured mechanical and thermal pain thresholds with and without unilateral photostimulation of STN neurons. We observed that 20 Hz photostimulation of STN neurons (*SI Appendix*, Fig. S4 *A* and *B*) dramatically reduced both the mechanical (Fig. 4*F*) and thermal (Fig. 4*G*) pain thresholds. Pain thresholds were unaffected by blue light illumination in mice that received a control AAV-CaMKII-eGFP injection in the STN (Fig. 4 *H* and *I*; *SI Appendix*, Fig. S4*B*).

We next examined the effects of STN photostimulation on neuronal activity in pain-processing nuclei. Our c-fos staining data reveal that unilateral optogenetic stimulation of STN neurons increased the numbers of c-fos–positive neurons in the prefrontal cortex, insular cortex, PBN, and pontine reticular nucleus in both hemispheres (*SI Appendix*, Fig. S5 *A*–*F*). These data suggest that the enhancement of neuronal activity in the unilateral STN may be adequate to sensitize bilateral pain-processing nuclei.

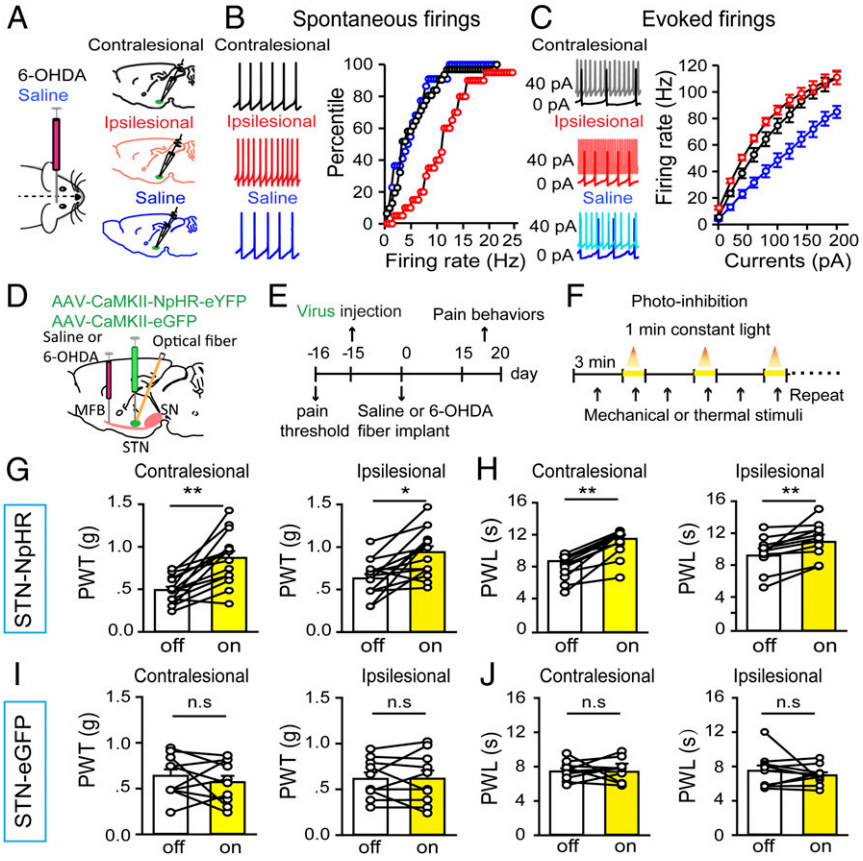

Fig. 2. Optogenetic inhibition of STN neurons rescues pain thresholds in parkinsonian mice. Pain behaviors were measured on postsurgery day 15. (*A*) Mice were subjected to injection of 6-OHDA or saline into the right MFB, and brain slices containing the STN were prepared for patch-clamp recordings. (*B*) Spontaneous firing (*Left*, representative traces) in contralesional and ipsilesional STN neurons from 6-OHDA lesioned mice and in ipsilateral STN neurons from saline-injected mice. There was a significant rightward shift in the percentile firing-rate curve for the ipsilesional side ($n = 20$ neurons; red) relative to the contralesional side ($n = 31$ neurons; black) and the saline group ($n = 20$ neurons; blue) (contralesional vs. ipsilesional: Kolmogorov–Smirnov K-S = 0.47, $P < 0.001$; Saline vs. ipsilesional: K-S = 0.51, $P < 0.001$; Saline vs. contralesional: K-S = 0.24, $P = 0.47$; K-S test). (*C*) Depolarizing current injection increased firing rates in STN neurons. (*Left*) Representative traces. (*Right*) Stimulation–response relationships of STN neurons on the ipsilesional side ($n = 10$ neurons; red), the contralesional side ($n = 16$ neurons; black), and in the Saline group ($n = 13$ neurons; blue) (among groups: $F = 15.49$, $P < 0.001$; currents: $F = 527.12$, $P < 0.001$; group × currents: $F = 5.38$, $P < 0.001$; two-way repeated measures ANOVA). (*D*) The viral vector AAV-CaMKII-NpHR3.0-eYFP or AAV-CaMKII-eGFP was injected into the STN of the right hemisphere, and an optical fiber was inserted above the injection site for optogenetic inhibition. 6-OHDA was injected into the MFB (ipsilateral to the virus injection) to establish a unilateral parkinsonian model. (*E*) Timeline of experiments. (*F*) STN neurons were photoinhibited by shining yellow light (3 mW for 1 min) through the optical implants, and mechanical and thermal pain thresholds were measured with von Frey filaments and a plantar anesthesia tester, respectively. (*G* and *H*) Optogenetic inhibition of STN neurons elevated mechanical pain threshold (*G*, *Left*, contralesional hindpaw: $n = 15$, $t = -5.48$, $P = 0.0001$; *Right*, ipsilesional hindpaw: $n = 15$, $t = -4.16$, $P = 0.001$; paired t test) and thermal pain threshold (*H*, *Left*, contralesional hindpaw: $n = 11$, $t = -6.87$, $P < 0.001$; *Right*, ipsilesional hindpaw: $n = 11$, $t = -3.88$, $P = 0.003$; paired t test) on both sides. (*I* and *J*) Yellow light stimulation of eGFP-expressing STN neurons changed neither the mechanical pain threshold (*I*, *Left*, contralesional hindpaw: $n = 10$, $t = -0.76$, $P = 0.47$; *Right*, ipsilesional hindpaw: $n = 10$, $t = -0.04$, $P = 0.97$; paired t test) nor the thermal pain threshold (*J*, *Left*, contralesional hindpaw: $n = 10$, $t = -0.07$, $P = 0.94$; *Right*, ipsilesional hindpaw: $n = 10$, $t = 0.84$, $P = 0.43$; paired t test) on either side. n.s., not statistically significant. $^*P < 0.05$; $^{**}P < 0.01$, light on vs. light off, paired t test.

Taken together, these results indicate that hyperactivity in STN neurons produced by direct neuromodulation is sufficient to promote activity in pain-processing nuclei and to induce pain hypersensitivity.

Optogenetic Stimulation of STN Neurons Recruits Downstream Nuclei to Reduce Pain Thresholds. We next applied morphological and optogenetic neuronal tracing techniques to reveal the neural circuits that mediate the regulation of pain by STN neurons. We used a transsynaptic neuronal tracer, wheat germ agglutinin (WGA), conjugated to Alexa Fluor 488, and observed fluorescently labeled downstream neurons of the STN (*SI Appendix*, Fig. S6 *A* and *B*) in the globus pallidus externa (GPe), globus pallidus interna (GPi), primary motor cortex (M1), PBN, pedunculopontine tegmental nucleus (PPN), substantia nigra pars compacta (SNc), substantia nigra pars reticulata (SNr), and ventral pallidum (VP) (*SI Appendix*, Fig. S6*C*). The data are consistent with previous neuroanatomic studies (25) and with the multiple physiological functions in which the STN is implicated, including motor control, reward processing, associative learning, and pain perception (16, 27). We also combined optogenetics and brain slice patch-clamp recordings to confirm that the upstream STN neurons formed functional glutamatergic synapses with SNr, GPi, and VP neurons, which were strong enough to enhance the activity of these neurons (*SI Appendix*, Fig. S6 *D–I*). These synaptic connections were also demonstrated by c-fos staining of these downstream neurons after in vivo blue light stimulation of the STN (*SI Appendix*, Fig. S7 *A–H*).

To address whether individual STN projections differentially mediate pain modulation, we optogenetically stimulated STN projections to the SNr, GPi, and VP (Fig. 5*A*) while measuring the mechanical and thermal pain thresholds. We observed that

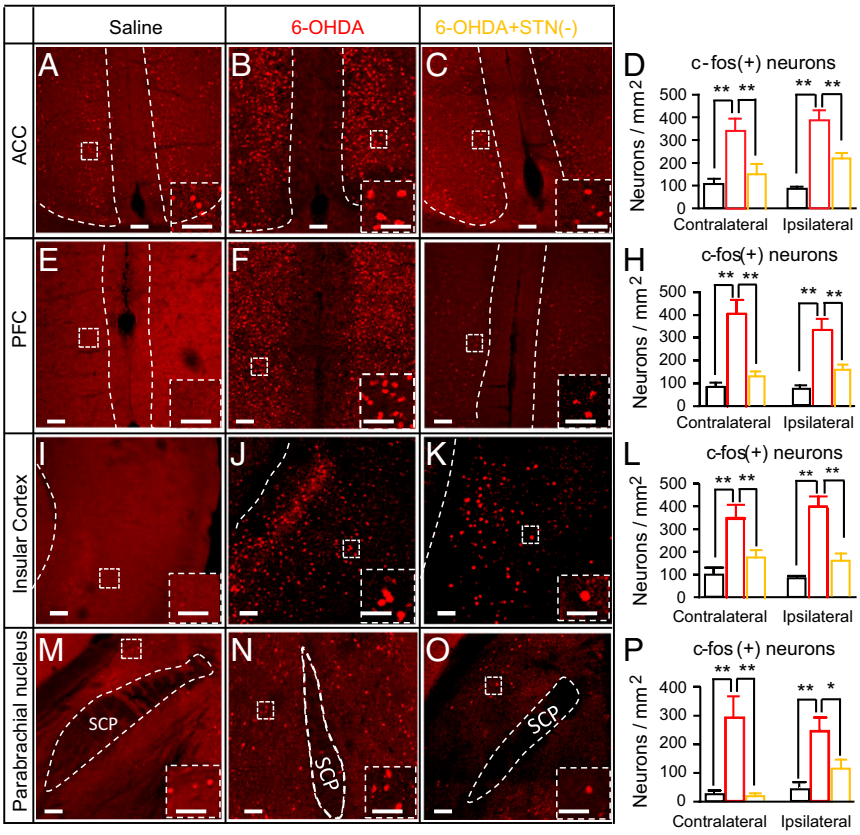

Fig. 3. Optogenetic inhibition of STN neurons reverses the hyperactivity in pain pathways in parkinsonian mice. Mice were divided into three groups that received saline (Saline) or 6-OHDA (6-OHDA) injection in the right MFB or a combination of 6-OHDA injection in the right MFB and optogenetic inhibition of ipsilesional STN neurons [6-OHDA+STN(–)]. The 6-OHDA+STN(–) mice were killed at 1 h after yellow light stimulation (2 min on/2 min off for 30 min). The number of c-fos–positive neurons differed among the three groups (3 mice each) in the cingulate cortex (*A–C*), prefrontal cortex (*E–G*), insular cortex (*I–K*), and PBN (*M–O*). (*D*) Summary of c-fos–positive neurons in the cingulate cortex. Contralesional, among groups: $F = 37.9$, $P < 0.001$; Saline vs. 6-OHDA: $t = 8.47$, $P < 0.001$; 6-OHDA vs. 6-OHDA+STN(–): $t = 6$, $P = 0.002$; ipsilesional, among groups: $F = 27.9$, $P < 0.001$; Saline vs. 6-OHDA: $t = 7.29$, $P = 0.001$; 6-OHDA vs. 6-OHDA+STN(–): $t = 5.04$, $P = 0.005$. (*H*) Summary of c-fos–positive neurons in the prefrontal cortex. Contralesional, among groups: $F = 25.1$, $P = 0.001$; Saline vs. 6-OHDA: $t = 6.6$, $P = 0.002$; 6-OHDA vs. 6-OHDA+STN(–): $t = 5.6$, $P = 0.003$; ipsilesional, among groups: $F = 19.7$, $P = 0.002$; Saline vs. 6-OHDA: $t = 6.1$, $P = 0.003$; 6-OHDA vs. 6-OHDA+STN(–): $t = 4.0$, $P = 0.01$. (*L*) Summary of c-fos–positive neurons in the insular cortex. Contralesional, among groups: $F = 10.8$, $P = 0.005$; Saline vs. 6-OHDA: $t = 4.4$, $P = 0.007$; 6-OHDA vs. 6-OHDA+STN(–): $t = 3.39$, $P = 0.02$; ipsilesional, among groups: $F = 27.4$, $P < 0.001$, Saline vs. 6-OHDA: $t = 6.6$, $P < 0.001$; 6-OHDA vs. 6-OHDA+STN(–): $t = 5.2$, $P = 0.003$. (*P*) Summary of c-fos–positive neurons in the PBN. Contralesional, among groups: $F = 17.5$, $P = 0.001$; Saline vs. 6-OHDA: $t = 5.36$, $P = 0.002$; 6-OHDA vs. 6-OHDA+STN(–): $t = 5.1$, $P = 0.002$; ipsilesional, among groups: $F = 8.68$, $P = 0.01$; Saline vs. 6-OHDA: $t = 4.0$, $P = 0.01$; 6-OHDA vs. 6-OHDA+STN(–): $t = 2.9$, $P = 0.04$. In the bar charts, Saline is in black, 6-OHDA is in red, and 6-OHDA+STN(–) is in orange; $^*P < 0.05$, $^{**}P < 0.01$, one-way ANOVA. (Scale bars: 100 μm in main images and 50 μm in insets.)

unilateral optogenetic stimulation of the STN-SNr (Fig. 5 *B* and *C*), STN-GPi (Fig. 5 *F* and *G*), and STN-VP (Fig. 5 *J* and *K*; *SI Appendix*, Fig. S8 *A–I*) projections induced significant bilateral pain hypersensitivity. Interestingly, photostimulation of STN-SNr projections reduced the thermal but not the mechanical pain threshold, whereas stimulation of STN-GPi and STN-VP projections reduced the mechanical but not the thermal pain threshold. In contrast, photostimulation did not alter pain thresholds in mice injected with AAV-CaMKII-eYFP in the STN and implanted with optical fibers in the SNr (Fig. 5 *D* and *E*), GPi (Fig. 5 *H* and *I*), and VP (Fig. 5 *L* and *M*). Note that mouse mobility in the chamber used for pain threshold measurement was not affected by photostimulation of STN-SNr, STN-GPi, or STN-VP projections (*SI Appendix*, Fig. S9 *A–F*).

These data indicate that STN neurons projection-specifically modulate thermal and mechanical pain thresholds. We propose that these patterns might have distinct circuit bases. According to our transsynaptic tracing data (*SI Appendix*, Fig. S10 *A–Q*), the profiles of brain regions innervated by the SNr and the VP were dramatically different. The former mainly projected to midbrain and brainstem structures, while the latter innervated forebrain, midbrain, and anterior brainstem structures. The activation of SNr, GPi, and VP neurons by photostimulation of STN terminals caused overactivation in the cingulate cortex, prefrontal cortex, primary somatosensory cortex, and insular cortex (*SI Appendix*, Fig. S11 *A–L*). Stimulation of STN-VP and STN-SNr projections induced stronger activation in the insular cortex and primary somatosensory cortex, respectively (*SI Appendix*, Fig. S11*M*). These findings support the notion that the distinct projection profiles of SNr, GPi, and VP neurons can confer their differential regulation of pain-processing pathways, leading to differential alteration of the thermal and mechanical pain thresholds.

Optogenetic Inhibition of Individual STN Projections Elevates Pain Thresholds in Parkinsonian Mice. Having demonstrated that the STN regulates pain perception through its projections to multiple nuclei (Fig. 5), we next asked whether these projections are functionally involved in pain hypersensitivity in parkinsonian mice (Fig. 2). To address this question, we optogenetically inhibited STN projections to the SNr (Fig. 6*A*), GPi (Fig. 6*D*), and VP (Fig. 6*G*; *SI Appendix*, Fig. S12 *A–C*, *E–G*, and *I–K*) in parkinsonian mice. We observed that photoinhibition of STN-SNr

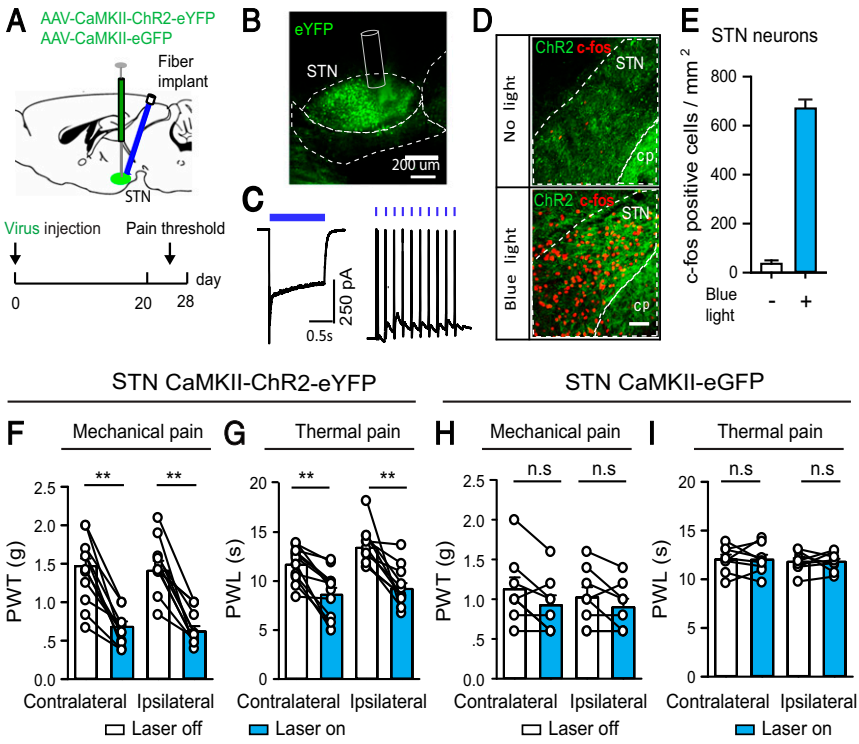

Fig. 4. Optogenetic stimulation of STN neurons induces pain hypersensitivity in mice. (*A*) Viral vector AAV-CaMKII-ChR2-eYFP or AAV-CaMKII-eGFP was injected into the right STN, and an optical fiber was inserted above the injection site for optogenetic stimulation. (*B–E*) The expression of ChR2-eYFP in STN neurons was confirmed by green fluorescent illumination (*B*; parasagittal section), brain slice patch-clamp recordings (*C*) in voltage-clamp mode (at −50 mV, *Left*) and current-clamp mode (*Right*), and c-fos staining of photostimulated STN (*D*, coronal sections, and *E*, summary). (*F–I*) STN neurons were photostimulated by shining blue light (10-ms pulse, 20 Hz, 4 mW, for 1 min) through the optical implant, and mechanical and thermal pain thresholds were measured with von Frey filaments and a plantar anesthesia tester, respectively. Optogenetic stimulation of STN neurons reduced the mechanical pain threshold (*F*, *Left*: contralateral hindpaw, $n = 11$, $t = 7.38$, $P < 0.001$; *Right*: ipsilateral hindpaw, $n = 12$, $t = 7.05$, $P < 0.001$) and thermal pain threshold (*G*, *Left*: contralateral hindpaw, $n = 12$, $t = 5.5$, $P < 0.001$; *Right*: ipsilateral hindpaw, $n = 12$, $t = 5.1$, $P < 0.001$) on both sides. Blue light illumination of eGFP-expressing STN neurons changed neither the mechanical pain threshold (*H*, *Left*: contralateral hindpaw, $n = 8$, $t = 2.37$, $P = 0.05$; *Right*: ipsilateral hindpaw, $n = 8$, $t = 1.67$, $P = 0.14$) nor the thermal pain threshold (*I*, *Left*: contralateral hindpaw, $n = 8$, $t = 0.07$, $P = 0.94$; *Right*: ipsilateral hindpaw, $n = 8$, $t = 0.003$, $P = 0.99$). $^{**}P < 0.01$; n.s., not statistically significant, light on vs. light off, paired *t* test. (Scale bars: 100 μm.)

projections attenuated both mechanical (Fig. 6*B*) and thermal (Fig. 6*C*) pain hypersensitivity, and that photoinhibition of STN-GPi and STN-VP projections attenuated mechanical (Fig. 6 *E* and *H*), but not thermal (Fig. 6 *F* and *I*), pain hypersensitivity. In this set of experiments, we did not observe any significant alterations in the mobility of these mice on yellow light illumination (*SI Appendix*, Fig. S12 *D*, *H*, and *L*), indicating that the increase in pain thresholds on optogenetic inhibition did not arise from dysfunction in voluntary movement.

Discussion

Although the STN responds to nociceptive stimulation (27, 35), no previous studies have performed reversible cell-specific neuromodulation to address whether and how STN neurons regulate pain in PD. In the present study, we combined electrophysiological techniques and optogenetic manipulations to demonstrate that reversing hyperactivity in STN neurons significantly attenuates pain hypersensitivity in parkinsonian mice. This result suggests that inhibiting STN neurons may be a potential therapeutic strategy for treating pain symptoms in PD. Because selective activation of D_2-like receptors reduces spontaneous firing rates in STN neurons (17), clinically available dopamine receptor agonists that have a high affinity to D_2-like receptors, such as L-dopa (a dopamine precursor), apomorphine, pramipexole, and rotigatine, also may inhibit STN neurons. Although these dopamine receptor agonists are administered systemically and their beneficial effects on pain symptoms in PD patients may be mediated by multiple neuronal populations (2, 7, 8, 36, 37), our data reveal that direct inhibition of STN neurons is sufficient to alleviate parkinsonian pain hypersensitivity.

Accumulating evidence shows that STN DBS effectively relieves musculoskeletal and dystonic pain in PD patients (28–32). Whether DBS at therapeutic frequencies causes inhibition or stimulation of STN neurons remains controversial (15, 16, 38, 39); therefore, the antinociceptive effect of STN DBS in PD patients cannot be directly linked to inhibition of STN neurons. Empirically, the direct targets of DBS (50 to 100 μs) are axonal fibers (40). Modulating synaptic inputs from the motor cortex and the PBN to the STN respectively mitigates motor deficits (26, 41) and nociceptive responses (27) in parkinsonian animals. Further investigations are warranted to elucidate whether STN neurons receiving different synaptic inputs differentially regulate motor functions and pain perception under both physiological and parkinsonian conditions, as well as whether they respond differentially to DBS.

Note that to reduce the mortality rate in mice, we used a partial parkinsonian model in which we injected 6-OHDA in the anterior part of the MFB (*SI Appendix*, Fig. S1), causing only a 50 to 60% loss of SNc DA neurons. In these partial parkinsonian mice, we observed moderate to mild motor deficits and pain hypersensitivity in the hindpaws. This is similar to the finding that some PD patients exhibit pain symptoms before motor dysfunction becomes noticeable (2). In addition to pain hypersensitivity, we also observed neuronal hyperactivity in the STN

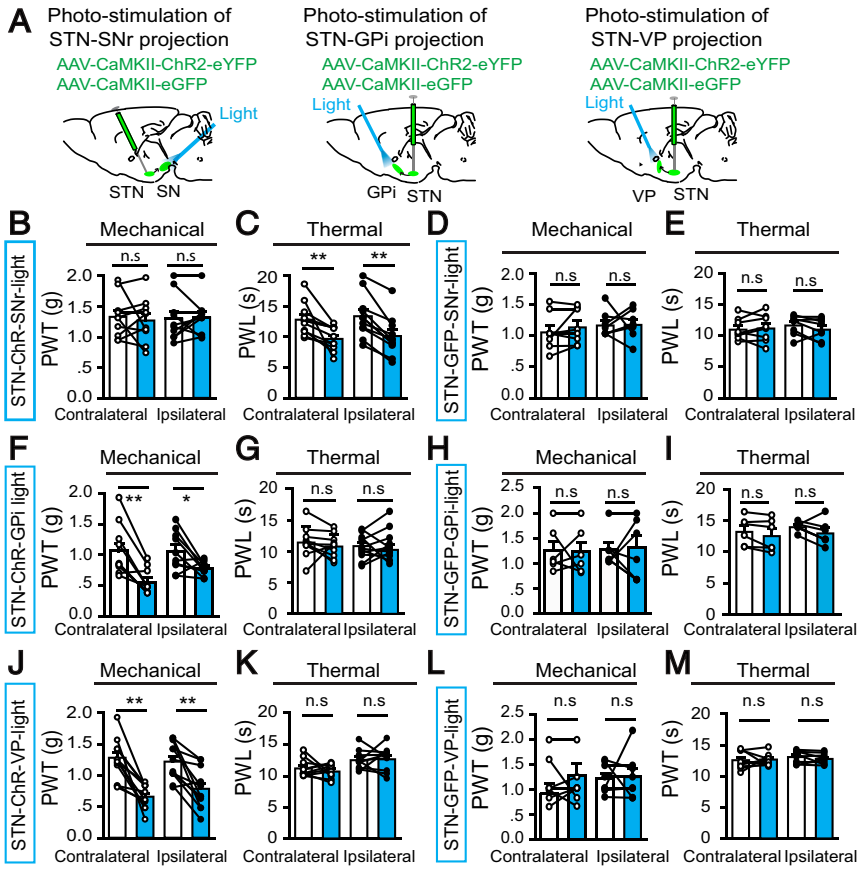

Fig. 5. Optogenetic stimulation of specific STN projections differentially reduces the mechanical and thermal pain thresholds. (*A*) AAV-CaMKII-ChR2-eYFP or AAV-CaMKII-eGFP was injected into the right STN, and optical fibers were implanted in the SNr, GPi, or VP ipsilateral to the viral injection. At 6 wk after viral injection, mechanical and thermal pain thresholds were measured with von Frey filaments and a plantar analgesia tester, respectively. (*B* and *C*) Blue light (473 nm, 10 ms, 20 Hz, 4 mW) was delivered for 1 min to photostimulate the axonal terminals of STN neurons, and the pain threshold assays were performed before the onset of the light and 30 to 60 s after the initiation of light delivery. Photostimulation of STN-SNr projections did not affect the mechanical pain threshold (*B*, contralateral hindpaw: $n = 10$, $t = 0.54$, $P = 0.6$; ipsilateral hindpaw: $n = 10$, $t = -0.28$, $P = 0.79$), but reduced the thermal pain threshold (*C*, contralateral hindpaw: $n = 10$, $t = 3.68$, $P = 0.005$; ipsilateral hindpaw: $n = 10$, $t = 6.31$, $P = 0.0007$). (*D* and *E*) Blue light delivery in the SNr of mice receiving the control AAV-CaMKII-eGFP injection had no effect on the mechanical pain threshold (*D*, contralateral hindpaw: $n = 8$, $t = -1.1$, $P = 0.29$; ipsilateral hindpaw: $n = 8$, $t = -0.13$, $P = 0.19$) or the thermal pain threshold (*E*, contralateral hindpaw: $n = 8$, $t = 0.38$, $P = 0.72$; ipsilateral hindpaw: $n = 8$, $t = 1.5$, $P = 0.17$). (*F* and *G*) Photostimulation of STN-GPi projections reduced the mechanical pain threshold (*F*, contralateral hindpaw: $n = 10$, $t = 5.43$, $P = 0.001$; ipsilateral hindpaw: $n = 10$, $t = 2.7$, $P = 0.02$), but not the thermal pain threshold (*G*, contralateral hindpaw: $n = 10$, $t = 0.9$, $P = 0.39$; ipsilateral hindpaw, $n = 10$, $t = -0.03$, $P = 0.98$). (*H* and *I*) Blue light delivery to the GPi of mice receiving the control AAV-CaMKII-eGFP injection had no effect on the mechanical pain threshold (*H*, contralateral hindpaw: $n = 6$, $t = 0.12$, $P = 0.91$; ipsilateral hindpaw: $n = 6$, $t = -0.17$, $P = 0.78$) or thermal pain threshold (*I*, contralateral hindpaw: $n = 6$, $t = 2.11$, $P = 0.09$; ipsilateral hindpaw: $n = 6$, $t = 1.45$, $P = 0.21$). (*J* and *K*) Photostimulation of STN-VP projections reduced the mechanical pain threshold (*J*, contralateral hindpaw: $n = 12$, $t = 6.36$, $P = 0.0005$; ipsilateral hindpaw: $n = 12$, $t = 4.43$, $P = 0.001$) but not the thermal pain threshold (*K*, contralateral hindpaw: $n = 12$, $t = 0.88$, $P = 0.41$; ipsilateral hindpaw: $n = 12$, $t = -0.22$, $P = 0.83$). (*L* and *M*) Blue light delivery to the VP of mice receiving the control AAV-CaMKII-eYFP injection did not change the mechanical pain threshold (*L*, contralateral hindpaw: $n = 8$, $t = 0.29$, $P = 0.78$; ipsilateral hindpaw: $n = 8$, $t = -0.18$, $P = 0.86$) or the thermal pain threshold (*M*, contralateral hindpaw: $n = 8$, $t = -0.19$, $P = 0.86$; ipsilateral hindpaw: $n = 8$, $t = 1.08$, $P = 0.32$). $^*P < 0.05$; $^{**}P < 0.01$; n.s., not statistically significant, light on vs. light off, paired *t* test. Locations of the tips of the optical implants are shown in *SI Appendix*, Fig. S8.

and overactivation of multiple pain-processing nuclei in these partial parkinsonian mice. Although previous individual studies have reported one or two of these events in PD (7, 8, 12–14, 16, 17), none has revealed a causal relationship between the hyperactivity of the STN in PD and pain hypersensitivity/enhanced activity in pain-processing nuclei. Using bidirectional optogenetic modulation, we demonstrated that the hyperactivity of STN neurons may be a major cause of these two events.

Previous studies on the involvement of the basal ganglia in pain processing have mostly focused on neurons in the striatum, globus pallidus, and substantia nigra (2, 10, 18). Our results reveal that hyperactivity of STN neurons sensitizes central pain-processing nuclei and causes pain hypersensitivity. In a positron emission tomography study in PD patients, L-dopa dramatically reduced pain responses in central pain-processing nuclei, including the anterior cingulate cortex, insular cortex, and prefrontal cortex (7). Our data suggest that inhibition of STN neurons may be another strategy to blunt the sensitivity of the central pain-processing nuclei in PD.

We also characterized the excitability of STN neurons in dopamine-depleted mice. First, ipsilesional STN neurons displayed higher spontaneous firing rates than contralesional STN neurons and STN neurons in control mice. This may be related to resting-state hyperactivity in central pain pathways. Second, in 6-OHDA lesioned mice, bilateral STN neurons exhibited overactivation in response to depolarizing stimulation relative to control mice. As stimulation of STN neurons reduces pain thresholds (Fig. 4) and STN neurons are excited by nociceptive stimulation (27, 35), the hyperresponsiveness of STN neurons in PD may initiate an exacerbation loop and strengthen the pain

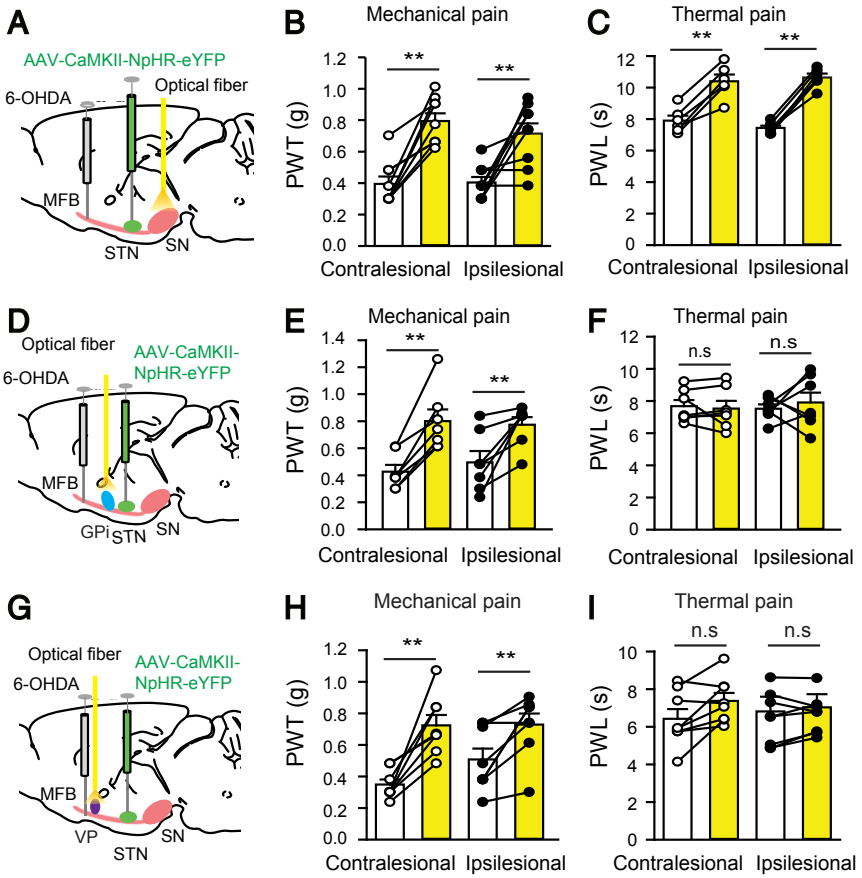

Fig. 6. Optogenetic inhibition of STN projections rescues the mechanical and thermal pain thresholds in parkinsonian mice. AAV-CaMKII-NpHR3.0-eYFP was injected into the right STN, 6-OHDA was injected into the MFB ipsilateral to the viral injection, and an optical fiber was implanted in the right SNr (*A*), GPi (*D*), or VP (*G*), and pain thresholds and mobility were measured 2 wk later. (*B* and *C*) Photoinhibition of the STN-SNr projection increased the mechanical pain threshold (*B*, contralesional hindpaw: $n = 9$, $t = -6.14$, $P = 0.001$; ipsilesional hindpaw: $n = 9$, $t = -3.64$, $P = 0.007$) and the thermal pain threshold (*C*, contralesional hindpaw: $n = 9$, $t = -8.18$, $P = 0.001$; ipsilesional hindpaw: $n = 9$, $t = -14.3$, $P = 0.001$). (*E* and *F*) Photoinhibition of the STN-GPi projection increased the mechanical pain threshold (*E*, contralesional hindpaw: $n = 7$, $t = -6.26$, $P = 0.001$; ipsilesional hindpaw: $n = 7$, $t = -3.6$, $P = 0.01$) but did not change the thermal pain threshold (*F*, contralesional hindpaw: $n = 7$, $t = 0.52$, $P = 0.63$; ipsilesional hindpaw: $n = 7$, $t = -0.57$, $P = 0.59$). (*H* and *I*) Photoinhibition of the STN-VP projection increased the mechanical pain threshold (*H*, contralesional hindpaw: $n = 8$, $t = -5.16$, $P = 0.001$; ipsilesional hindpaw: $n = 8$, $t = -3.72$, $P = 0.008$), but did not change the thermal pain threshold (*I*, contralesional hindpaw: $n = 8$, $t = -2.67$, $P = 0.03$; ipsilesional hindpaw: $n = 8$, $t = -1.11$, $P = 0.3$). $^*P < 0.05$; $^{**}P < 0.01$; n.s., not statistically significant, light on vs. light off, paired *t* test. Locations of the tips of the optical implants are shown in *SI Appendix*, Fig. S12.

experience. Because the STN and SNc have few contralateral projections (25), the enhanced excitability of contralesional STN neurons may be the result of neuroadaptation. Therefore, the elevation of pain thresholds in parkinsonian mice by inhibition of STN neurons may occur via mitigation of hyperactivity in central pain pathways and elimination of an STN-related exacerbation loop for nociceptive signaling. In control mice, activation of the central pain pathway by the STN is limited; thus, inhibition of STN neurons in these mice may not lead to reductions in the activity level in central pain pathways, resulting in only minor effects on pain thresholds.

The SNr, GPi, and VP are involved in the perception of multiple types of nociceptive stimuli (10, 18, 42). We found that SNr, GPi, and VP neurons receiving STN projections differentially regulate mechanical and thermal pain thresholds in both control and parkinsonian mice, suggesting that subpopulations of STN projection neurons may be effective therapeutic targets for the treatment of diverse pain symptoms in PD. The involvement of the STN-GPi pathway in the perception of mechanical sensory stimulation provides an explanation for clinical observations that either pallidotomy or pallidal DBS, which may disrupt STN-GPi transmission, relieves pain symptoms in PD, including dyskinetic, dystonic, and musculoskeletal pain (43, 44). Although it has been shown that both SNr and VP neurons respond to painful stimuli (2, 10, 18, 42), our results are among the first to hint at the critical roles of these two nuclei in parkinsonian pain hypersensitivity. The fact that STN DBS mitigates musculoskeletal and dystonic pain better than central and radicular/neuropathic pain (28) further suggests that the STN may regulate the perception of distinct types of pain stimuli. Therefore, our data imply that abnormal activity in subpopulations of STN projection neurons may be important pathophysiological components in the basal ganglia associated with distinct sensory symptoms in PD.

Our neuronal tracing data support the hypothesis that the STN directly modulates the PBN but indirectly modulates the insular cortex, cingulate cortex, and prefrontal cortex. Among these nuclei, the posterior and anterior insular cortices are involved in coding the sensory discriminative and emotional components of pain, respectively, whereas the other nuclei contribute to the emotional and motivational components of pain (45–48). These brain regions are differentially activated during heat and mechanical hyperalgesia (48). Our transsynaptic tracing and c-fos staining data support the hypothesis that the distinct projection profiles of the SNr, GPi, and VP may introduce

variations in the representation of pain in brain regions that encode sensory discrimination; however, sophisticated transsynaptic neuronal tracing, projection-specific neuromodulation, and pain behavioral studies are needed to elucidate the neural circuits.

In the present study, we observed that unilateral lesion of SNc DA neurons reduced nociceptive thresholds bilaterally in mice, similar to previous findings in unilateral 6-OHDA lesioned rats (49–51). Significant bilateral pain symptoms have also been reported in PD patients with unilateral motor deficits (52, 53). Abnormal activity in the SNr, GPi, and STN in PD animals and patients (11–17) can be associated with bilateral pain hypersensitivity in PD. Early in vivo electrophysiological studies delineated sensory receptive fields of neurons in the substantia nigra, globus pallidus, and ventral pallidum and found that approximately one-half of the neurons in these nuclei responded to stimulation in large areas on both the ipsilateral and contralateral sides (10). In this scenario, dysfunction of the basal ganglia nuclei in one hemisphere may affect pain signaling on both sides. In the present study, to mimic the hyperactivity of STN neurons observed in the parkinsonian state, we applied optogenetic stimulation to the STN unilaterally. This unilateral stimulation activated central pain-processing nuclei in both hemispheres and reduced pain thresholds in both hindpaws. Therefore, we postulate that unilateral dopamine depletion leads to abnormal activity in the basal ganglia neurons, with the latter followed by sensitization of bilateral central pain-processing nuclei and bilateral pain hypersensitivity.

In summary, this study demonstrates that in parkinsonian mice, hyperactivity of STN neurons is causally linked to pain hypersensitivity. We found that hyperactivity of STN neurons sensitized the central pain processing nuclei and led to pain hypersensitivity, whereas inhibition of STN neurons eliminated hyperactivity in central pain-processing nuclei and attenuated the associated pain hypersensitivity. Furthermore, the STN projections to the SNr, GPi, and VP differentially regulated mechanical and thermal pain thresholds. Therefore, inhibition of STN neurons or particular STN projections may be promising therapeutic strategies for the treatment of distinct pain phenotypes in PD.

Materials and Methods

Animals. The care and use of animals and the experimental protocols used in this study were approved by the Institutional Animal Care and Use Committee and the Office of Laboratory Animal Resources of Xuzhou Medical University. Male C57BL/6 mice (2–6 mo old) were group-housed (≤ 4 per cage) on a 12-h light/dark cycle. The mice had free access to water and food. The mice were randomly allocated into the groups described in the following experiments. Efforts were made to minimize animal suffering and to reduce the numbers of animals used. See *SI Appendix* for details.

AAV Vectors. The viral vectors, including AAV-CaMKII-EGFP, AAV-CaMKII-hChR2 (H134R)-YFP, and AAV-CaMKII-NpHR3.0-eYFP (serotype 2; 1×10^{12} to 5×10^{12} vg/mL), were purchased from OBIO Technology or Brain VTA).

Surgical Procedures. Mice (3 to 4 mo old, 25 to 30 g) were anesthetized with sodium pentobarbital and stabilized in a stereotaxic frame (RWD Life Science). They were then subjected to unilateral 6-OHDA (0.3 μL, 15 μg/μL; Tocris) microinjection into the MFB, viral vector delivery (0.3 μL), optical fiber implantation, and transsynaptic neuronal tracing (WGA 0.1 μL, 1 μg/μL; Thermo Fisher Scientific). Details are provided in *SI Appendix*.

Electrophysiological Recordings. To verify that the virus was functional, we performed patch-clamp recordings in brain slices using a modified version of a previously described protocol (17, 54), as described in detail in *SI Appendix*.

Behavioral Tests. Individual mice were placed in test chambers ($7.5 \times 7.5 \times 15$ cm^3, LWH) with no bottom or cover on a wide-gauge wire mesh supported by an elevated platform. After at least 30 min of habituation, mechanical pain thresholds were measured in mice with von Frey filaments and the up-down method (55). The 50% paw withdrawal threshold (PWT) was determined as described previously (56). Motor behavior was recorded with a video camera controlled by EthoVision XT 9 software (Noldus) (57, 58). Thermal paw withdrawal latencies (PWLs) were measured with a plantar anesthesia tester (Boerni). The results from three tests were averaged to represent the PWL for each mouse. More detailed information is provided in *SI Appendix*.

Immunohistochemistry. Mice were killed with CO_2 and immediately subjected to cardiac perfusion with PBS, followed by 4% paraformaldehyde (PFA) in PBS. Brains were removed and postfixed in PFA for 12 h at 4 °C. Brain sections (50 μm) were cut on a vibratome and mounted onto glass slides. Immunostaining and microscopy were performed with a standard protocol (17, 58), as described in detail in *SI Appendix*.

Confocal Microscopy. Low- and high-magnification images were acquired with a Zeiss LSM 880 confocal microscope, controlled by Zen2 acquisition software (Zeiss). The images were processed with Image J (59). *SI Appendix* provides more details.

Statistical Analysis. SigmaPlot version 14.0 (SPSS) was used for all statistical analyses. Details are provided in *SI Appendix*.

Data Availability Statement. All data discussed in the paper are available in the *SI Appendix*.

ACKNOWLEDGMENTS. This work was supported by the National Natural Science Foundation of China (81701100, to C.Z.; 81870891, to C.X.; 81971038, to C.Z.; 31771161, to J.C.; and 8172010801, to J.C.), the Fund for Jiangsu Province Specially Appointed Professors (C.X. and C.Z.), the Natural Science Foundation of Jiangsu Province (BK20171160, to C.Z.), The Natural Science Foundation of the Jiangsu Higher Education Institutions of China (17KJA320007 to C.X. and 18KJA320009, to C.Z.), the Jiangsu Province Fund for Dominant Discipline (Anesthesiology), and Startup Funds from Xuzhou Medical University (D2017009 and D2017010).

1. A. G. Beiske, J. H. Loge, A. Rønningen, E. Svensson, Pain in Parkinson's disease: Prevalence and characteristics. *Pain* **141**, 173–177 (2009).
2. P. J. Blanchet, C. Brefel-Courbon, Chronic pain and pain processing in Parkinson's disease. *Prog. Neuropsychopharmacol. Biol. Psychiatry* **87**, 200–206 (2018).
3. M. P. Broen, M. M. Braaksma, J. Patijn, W. E. Weber, Prevalence of pain in Parkinson's disease: A systematic review using the modified QUADAS tool. *Mov. Disord.* **27**, 480–484 (2012).
4. G. Wasner, G. Deuschl, Pains in Parkinson disease—Many syndromes under one umbrella. *Nat. Rev. Neurol.* **8**, 284–294 (2012).
5. A. J. Lees, J. Hardy, T. Revesz, Parkinson's disease. *Lancet* **373**, 2055–2066 (2009).
6. H. Bergman, G. Deuschl, Pathophysiology of Parkinson's disease: From clinical neurology to basic neuroscience and back. *Mov. Disord.* **17** (suppl. 3), S28–S40 (2002).
7. C. Brefel-Courbon *et al.*, Effect of levodopa on pain threshold in Parkinson's disease: A clinical and positron emission tomography study. *Mov. Disord.* **20**, 1557–1563 (2005).
8. A. Gerdelat-Mas *et al.*, Levodopa raises objective pain threshold in Parkinson's disease: A RIII reflex study. *J. Neurol. Neurosurg. Psychiatry* **78**, 1140–1142 (2007).
9. K. Seppi *et al.*; the collaborators of the Parkinson's Disease Update on Non-Motor Symptoms Study Group on behalf of the Movement Disorders Society Evidence-Based Medicine Committee, Update on treatments for nonmotor symptoms of Parkinson's disease: An evidence-based medicine review. *Mov. Disord.* **34**, 180–198 (2019).
10. E. H. Chudler, W. K. Dong, The role of the basal ganglia in nociception and pain. *Pain* **60**, 3–38 (1995).
11. D. S. Kreiss, C. W. Mastropietro, S. S. Rawji, J. R. Walters, The response of subthalamic nucleus neurons to dopamine receptor stimulation in a rodent model of Parkinson's disease. *J. Neurosci.* **17**, 6807–6819 (1997).
12. H. Bergman, T. Wichmann, B. Karmon, M. R. DeLong, The primate subthalamic nucleus, II: Neuronal activity in the MPTP model of parkinsonism. *J. Neurophysiol.* **72**, 507–520 (1994).
13. T. Wichmann, H. Bergman, M. R. DeLong, The primate subthalamic nucleus, III: Changes in motor behavior and neuronal activity in the internal pallidum induced by subthalamic inactivation in the MPTP model of parkinsonism. *J. Neurophysiol.* **72**, 521–530 (1994).
14. M. Magnin, A. Morel, D. Jeanmonod, Single-unit analysis of the pallidum, thalamus, and subthalamic nucleus in parkinsonian patients. *Neuroscience* **96**, 549–564 (2000).
15. J. S. Perlmutter, J. W. Mink, Deep brain stimulation. *Annu. Rev. Neurosci.* **29**, 229–257 (2006).
16. C. Hamani *et al.*, Subthalamic nucleus deep brain stimulation: Basic concepts and novel perspectives. *eNeuro* **4**, ENEURO.0140-17.2017 (2017).
17. C. Zhou *et al.*, Bidirectional dopamine modulation of excitatory and inhibitory synaptic inputs to subthalamic neuron subsets containing α4β2 or α7 nAChRs. *Neuropharmacology* **148**, 220–228 (2019).
18. D. Borsook, J. Upadhyay, E. H. Chudler, L. Becerra, A key role of the basal ganglia in pain and analgesia—Insights gained through human functional imaging. *Mol. Pain* **6**, 27 (2010).

19. W. Dieb, O. Ouachikh, F. Durif, A. Hafidi, Lesion of the dopaminergic nigrostriatal pathway induces trigeminal dynamic mechanical allodynia. *Brain Behav.* **4**, 368–380 (2014).
20. W. Dieb, O. Ouachikh, F. Durif, A. Hafidi, Nigrostriatal dopaminergic depletion produces orofacial static mechanical allodynia. *Eur. J. Pain* **20**, 196–205 (2016).
21. J. Park *et al*., Pain perception in acute model mice of Parkinson's disease induced by 1-methyl-4-phenyl-1,2,3,6-tetrahydropyridine (MPTP). *Mol. Pain* **11**, 28 (2015).
22. Y. Zengin-Toktas, J. Ferrier, F. Durif, P. M. Llorca, N. Authier, Bilateral lesions of the nigrostriatal pathways are associated with chronic mechanical pain hypersensitivity in rats. *Neurosci. Res.* **76**, 261–264 (2013).
23. A. C. P. Campos, M. B. Berzuino, M. S. Hernandes, E. T. Fonoff, R. L. Pagano, Monoaminergic regulation of nociceptive circuitry in a Parkinson's disease rat model. *Exp. Neurol.* **318**, 12–21 (2019).
24. E. E. Benarroch, Subthalamic nucleus and its connections: Anatomic substrate for the network effects of deep brain stimulation. *Neurology* **70**, 1991–1995 (2008).
25. E. Marani, T. Heida, E. A. Lakke, K. G. Usunoff, The subthalamic nucleus. Part I: Development, cytology, topography and connections. *Adv. Anat. Embryol. Cell Biol.* **198**, 1–113, vii (2008).
26. V. Gradinaru, M. Mogri, K. R. Thompson, J. M. Henderson, K. Deisseroth, Optical deconstruction of parkinsonian neural circuitry. *Science* **324**, 354–359 (2009).
27. A. Pautrat *et al*., Revealing a novel nociceptive network that links the subthalamic nucleus to pain processing. *eLife* **7**, e36607 (2018).
28. R. G. Cury *et al*., Effects of deep brain stimulation on pain and other nonmotor symptoms in Parkinson disease. *Neurology* **83**, 1403–1409 (2014).
29. J. Gierthmühlen *et al*., Influence of deep brain stimulation and levodopa on sensory signs in Parkinson's disease. *Mov. Disord.* **25**, 1195–1202 (2010).
30. Y. J. Jung *et al*., An 8-year follow-up on the effect of subthalamic nucleus deep brain stimulation on pain in Parkinson disease. *JAMA Neurol.* **72**, 504–510 (2015).
31. H. J. Kim, B. S. Jeon, S. H. Paek, Nonmotor symptoms and subthalamic deep brain stimulation in Parkinson's disease. *J. Mov. Disord.* **8**, 83–91 (2015).
32. J. Pellaprat *et al*., Deep brain stimulation of the subthalamic nucleus improves pain in Parkinson's disease. *Parkinsonism Relat. Disord.* **20**, 662–664 (2014).
33. M. A. Cenci, M. Lundblad, Ratings of L-DOPA–induced dyskinesia in the unilateral 6-OHDA lesion model of Parkinson's disease in rats and mice. *Curr. Protoc. Neurosci.* Chapter 9, Unit 9.25 (2007).
34. K. Tieu, A guide to neurotoxic animal models of Parkinson's disease. *Cold Spring Harb. Perspect. Med.* **1**, a009316 (2011).
35. A. Belasen *et al*., The effects of mechanical and thermal stimuli on local field potentials and single unit activity in Parkinson's disease patients. *Neuromodulation* **19**, 698–707 (2016).
36. O. Skogar, J. Lokk, Pain management in patients with Parkinson's disease: Challenges and solutions. *J. Multidiscip. Healthc.* **9**, 469–479 (2016).
37. M. A. Stacy, H. Murck, K. Kroenke, Responsiveness of motor and nonmotor symptoms of Parkinson disease to dopaminergic therapy. *Prog. Neuropsychopharmacol. Biol. Psychiatry* **34**, 57–61 (2010).
38. S. Miocinovic, S. Somayajula, S. Chitnis, J. L. Vitek, History, applications, and mechanisms of deep brain stimulation. *JAMA Neurol.* **70**, 163–171 (2013).
39. J. L. Vitek, L. A. Johnson, Understanding Parkinson's disease and deep brain stimulation: Role of monkey models. *Proc. Natl. Acad. Sci. U.S.A.* 201902300 (2019).
40. P. Mazzone, E. Scarnati, E. Garcia-Rill, Commentary. The pedunculopontine nucleus: Clinical experience, basic questions and future directions. *J. Neural Transm. (Vienna)* **118**, 1391–1396 (2011).
41. T. H. Sanders, D. Jaeger, Optogenetic stimulation of cortico-subthalamic projections is sufficient to ameliorate bradykinesia in 6-OHDA lesioned mice. *Neurobiol. Dis.* **95**, 225–237 (2016).
42. A. B. Wulff, J. Tooley, L. J. Marconi, M. C. Creed, Ventral pallidal modulation of aversion processing. *Brain Res.* **1713**, 62–69 (2019).
43. C. R. Honey, A. J. Stoessl, J. K. Tsui, M. Schulzer, D. B. Calne, Unilateral pallidotomy for reduction of parkinsonian pain. *J. Neurosurg.* **91**, 198–201 (1999).
44. T. J. Loher, J. M. Burgunder, S. Weber, R. Sommerhalder, J. K. Krauss, Effect of chronic pallidal deep brain stimulation on off period dystonia and sensory symptoms in advanced Parkinson's disease. *J. Neurol. Neurosurg. Psychiatry* **73**, 395–399 (2002).
45. R. K. Hofbauer, P. Rainville, G. H. Duncan, M. C. Bushnell, Cortical representation of the sensory dimension of pain. *J. Neurophysiol.* **86**, 402–411 (2001).
46. C. Maihöfner, H. O. Handwerker, Differential coding of hyperalgesia in the human brain: A functional MRI study. *Neuroimage* **28**, 996–1006 (2005).
47. C. Maihöfner, B. Herzner, H. Otto Handwerker, Secondary somatosensory cortex is important for the sensory-discriminative dimension of pain: A functional MRI study. *Eur. J. Neurosci.* **23**, 1377–1383 (2006).
48. F. Seifert, I. Jungfer, M. Schmelz, C. Maihöfner, Representation of UV-B–induced thermal and mechanical hyperalgesia in the human brain: A functional MRI study. *Hum. Brain Mapp.* **29**, 1327–1342 (2008).
49. E. H. Chudler, Y. Lu, Nociceptive behavioral responses to chemical, thermal and mechanical stimulation after unilateral, intrastriatal administration of 6-hydroxydopamine. *Brain Res.* **1213**, 41–47 (2008).
50. L. E. Gee, N. Chen, A. Ramirez-Zamora, D. S. Shin, J. G. Pilitsis, The effects of subthalamic deep brain stimulation on mechanical and thermal thresholds in 6OHDA-lesioned rats. *Eur. J. Neurosci.* **42**, 2061–2069 (2015).
51. A. Gómez-Paz, R. Drucker-Colín, D. Milán-Aldaco, M. Palomero-Rivero, M. Ambriz-Tututi, Intrastriatal chromospheres' transplant reduces nociception in hemiparkinsonian rats. *Neuroscience* **387**, 123–134 (2018).
52. R. Djaldetti *et al*., Quantitative measurement of pain sensation in patients with Parkinson disease. *Neurology* **62**, 2171–2175 (2004).
53. G. D. Schott, Pain in Parkinson's disease. *Pain* **22**, 407–411 (1985).
54. C. Xiao *et al*., Nicotinic receptor subtype-selective circuit patterns in the subthalamic nucleus. *J. Neurosci.* **35**, 3734–3746 (2015).
55. C. Zhou, Z. D. Luo, Nerve injury-induced calcium channel alpha-2-delta-1 protein dysregulation leads to increased pre-synaptic excitatory input into deep dorsal horn neurons and neuropathic allodynia. *Eur. J. Pain* **19**, 1267–1276 (2015).
56. W. J. Dixon, Efficient analysis of experimental observations. *Annu. Rev. Pharmacol. Toxicol.* **20**, 441–462 (1980).
57. L. P. Noldus, A. J. Spink, R. A. Tegelenbosch, EthoVision: A versatile video tracking system for automation of behavioral experiments. *Behav. Res. Methods Instrum. Comput.* **33**, 398–414 (2001).
58. C. Xiao *et al*., Cholinergic mesopontine signals govern locomotion and reward through dissociable midbrain pathways. *Neuron* **90**, 333–347 (2016).
59. C. A. Schneider, W. S. Rasband, K. W. Eliceiri, NIH Image to Im: 25 years of image analysis. *Nat. Methods* **9**, 671–675 (2012).